HHS Public Access

Author manuscript

J Immunol. Author manuscript; available in PMC 2021 September 15.

Published in final edited form as:

J Immunol. 2020 September 15; 205(6): 1633–1643. doi:10.4049/jimmunol.2000440.

Identification of a novel anti-sepsis pathway: Sectm1a enhances macrophage phagocytosis of bacteria through activating GITR

Xingjiang Mu[*], **Peng Wang**[*,†], **Xiaohong Wang**[*], **Yutian Li**[*], **Hongyan Zhao**[*,‡], **Qianqian Li**[*,§], **Kobina Essandoh**[*], **Shan Deng**[*,¶], **Tianqing Peng**[#], **Guo-Chang Fan**[*]

[*] Pharmacology and Systems Physiology, University of Cincinnati College of Medicine; Cincinnati, OH 45267, USA

[†] Department of Critical Care Medicine, Shandong Provincial Hospital Affiliated to Shandong First Medical University, Jinan, Shandong, China

[‡] Department of Critical Care Medicine, the Second Hospital of Shandong University, Jinan, Shandong, China

[§] Division of Pharmaceutical Science, James L. Winkle College of Pharmacy, University of Cincinnati, Cincinnati, OH 45267, USA

[¶] Department of Cardiology, Union Hospital, Tongji Medical College, Huazhong University of Science and Technology, Wuhan, Hubei, 430022, China

[#] Critical Illness Research, Lawson Health Research Institute, Ontario N6A 4G5, Canada

Abstract

The inability to effectively control invading bacteria or other pathogens is a major cause of multiple organ dysfunction and death in sepsis. As the first-line defense of immune system, macrophages play a crucial role in the removal of pathogens during sepsis. In this study, we define secreted and transmembrane1A (Sectm1a) as a novel ligand of glucocorticoid-induced tumor necrosis factor receptor (GITR) that greatly boosts macrophage phagocytosis and bactericidal capacity. Using a global Sectm1a-knockout (KO) mouse model, we observed that Sectm1a deficiency significantly suppressed phagocytosis and bactericidal activity in both recruited macrophages and tissue-resident macrophages, which consequently aggravated bacterial burden in the blood and multiple organs, and further increased systemic inflammation, leading to multiple organ injury and increased mortality during polymicrobial sepsis. By contrast, treatment of septic mice with recombinant Sectm1a protein (rSectm1a) not only promoted macrophage phagocytosis and bactericidal activity but also significantly improved survival outcome. Mechanistically, we identified that Sectm1a could bind to GITR in the surface of macrophages and thereby activated its

1. Corresponding author: Guo-Chang Fan, PhD (fangg@ucmail.uc.edu), Department of Pharmacology and Systems Physiology, University of Cincinnati College of Medicine, 231 Albert Sabin Way, Cincinnati, OH 45267-0575. Phone: (513) 558-2340; Fax: (513) 558-9969.

2. Author contribution : X.M. designed, performed experiments, and wrote manuscript. P.W., H.Z. and Q.L. helped to sacrifice mice and collect samples. S. D. and Y.L. initially generated Sectm1a-KO mouse model. X.W. conducted Western-blotting experiments. Y.L. and K.E. reviewed/edited manuscript. T.P. helped to analyze data. G.-C. F. conceived the project, analyzed results, reviewed/edited manuscript, provided financial and administrative support, and gave final approval of the manuscript.

Conflict of interest statement:
The authors have declared that no conflict of interest exists.

downstream PI3K-Akt pathway. Accordingly, rSectm1a-mediated phagocytosis and bacterial killing were abolished in macrophages by either knockout of GITR or pharmacologically inhibition of the PI3K-Akt pathway. In addition, rSectm1a-induced therapeutic effects on sepsis injury were negated in GITR-KO mice. Taken together, these results uncover that Sectm1a may represent a novel target for drug development to control bacterial dissemination during sepsis or other infectious diseases.

Keywords

Sepsis; Macrophages; Phagocytosis; Bactericidal Activity; Sectm1a; GITR

Introduction

Despite many advances in various therapeutic approaches, sepsis remains a major clinic challenge worldwide and a huge burden across all economic regions (1). Recent studies reported that 31.5 million cases of sepsis and 19.4 million cases of severe sepsis occur annually in high-income countries (1, 2). In the United States, sepsis incidence has been increased by 8.7% per year during the past two decades (2). Notably, as the leading cause of mortality in intensive care units, sepsis accounts for more than 50% of hospital deaths and a considerable economic impact (13% of total U.S. hospital costs) (3, 4). New anti-inflammatory treatment strategies aiming to reduce mortality rate have been uniformly proven ineffective in clinical trials (5, 6). In addition, the emergence of multidrug-resistant bacteria further limits the efficacy of antibiotic therapy in septic patients (7). Therefore, it is urgently needed to develop alternative treatment strategies such as enhancing host defense to facilitate timely clearance of bacteria.

As the first-line defense during infection, innate immunity plays a crucial role in sepsis due to its immediate response to pathogens within minutes as a “rapid response team”. One of the most important initial innate immune defenses is the phagocytosis and internal killing of pathogens by phagocytic cells. Patients with defects in phagocytic function typically experience early dissemination of pathogens, leading to severe sepsis and increased mortality (8). It is reported that reduced phagocytic activity during the first 24 h after admission has been identified as a positive predictor for mortality in septic patients (9). As professional phagocytic cells, neutrophils and macrophages are vital to host defense against microorganisms due to their ability in internalizing and digesting bacteria, and scavenging toxic compounds produced by metabolism. Accumulating evidence has demonstrated that macrophages are the first cellular responders to bacterial infection, whereas neutrophils function as a backup system when the scavenging capacity of macrophages is overwhelmed in the situation of hyper-inflammation (10, 11). Indeed, the impairment of macrophage function has been reported to be primarily responsible for the insufficient antibacterial defenses and hyper-inflammation in sepsis (12). Thus, better understanding of macrophage function and the underlying molecular mechanism that regulates phagocytic capacity would be warranted for the development of more efficacious therapies.

In humans, Sectm1 (secreted and transmembrane 1), also referred to as K12, is highly expressed in cells of the myeloid lineage and epithelia (13, 14). It has been implicated as an alternative ligand of CD7 to co-stimulate T cell proliferation and IL-2 release (13, 14). Tsalik *et al.* recently sequenced peripheral blood RNA of 129 representative subjects with systemic inflammatory response syndrome (SIRS) or sepsis including 78 sepsis survivors and 28 sepsis non-survivors (15). They found that mRNA levels of Sectm1 were significantly lower in the blood cells of non-survivor sepsis patients compared to survivors (15). Similarly, our initial ELISA results demonstrated that sepsis patients had significantly lower levels of Sectm1 in the plasma compared to healthy donors (16). These results suggest that Sectm1 may play an important role in the pathogenesis of sepsis. Mouse Sectm1a shares the greatest homology to human Sectm1 (17, 18). In addition, mouse Sectm1a is also able to act as a co-stimulator of T cells to enhance T cell proliferation and IL-2 production; but such action is dependent on GITR (glucocorticoid-induced TNF receptor) activation rather than CD7 stimulation (18). Nevertheless, to our knowledge, the functional role of Sectm1a in macrophage phagocytosis during polymicrobial sepsis has never been investigated.

In this study, we firstly determined whether Sectm1a expression was altered in macrophages during polymicrobial sepsis. Next, we investigated the effects of Sectm1a deficiency in sepsis-induced bacterial burden, systemic inflammation, multiple organ injury and animal mortality. Furthermore, therapeutic role of recombinant Sectm1a protein in septic mice was also tested. Lastly, using GITR-KO mice, we explored the mechanism underlying Sectm1a-elicited beneficial effects.

Materials and methods

Mice

Wild-type (WT) and GITR-KO (Tnfrsf18$^{-/-}$) mice (both on the C57BL/6 background) were purchased from the Jackson Laboratory (Bar Harbor, ME, USA). The global Sectm1a-KO mouse model with C57BL/6 background was generated using CRISPR/Cas9 system and detailed in our recent publication (19). All mice were maintained and bred under specific pathogen-free conditions in the Division of Laboratory Animal Resources at the University of Cincinnati Medical Center. All animal experiments conformed to the Guidelines for the Care and Use of Laboratory Animals prepared by the National Academy of Sciences, published by the National Institutes of Health, and approved by the University of Cincinnati Animal Care and Use Committee. Male and female mice between 6 and 10 weeks of age were used for experiments in a gender-matched manner.

Polymicrobial sepsis model, survival and bacterial burden assay

Mouse polymicrobial sepsis was induced by cecal ligation puncture (CLP) using a 21-gauge needle as described previously (20). After surgery, mice were resuscitated by injecting subcutaneously 1 ml of pre-warmed 0.9% saline solution. For survival studies, male mice (7–8 weeks) were monitored every 6 hours for 4 days. Bacterial burden assay was performed as described previously (21). The peritoneal lavage fluid, blood samples, spleen and lung homogenates were collected at 24 h after CLP surgery, serially diluted in 10-fold with sterile

phosphate-buffered saline (PBS). Serial dilutions in PBS were plated onto TSA and grown overnight at 37°C, and colonies were counted.

Tissue wet-to-dry weight ratio

To quantify spleen and lung edema, whole spleen and lung tissues were collected, rinsed with PBS to remove surface blood and patted dry. The immediate weights of samples were recorded as wet weight. All tissues were air dried for 2 d at 60°C, and their weights were recorded as dry weight. A wet/dry weight ratio for each individual mouse was calculated.

Isolation of RNA and quantitative real-time PCR (qRT-PCR)

Total RNA was extracted from whole blood using RNA blood purification kit (Invitrogen, Carlsbad, CA, USA), and from tissues using the RNeasy kit (Qiagen) following the manufacturer's manual. cDNA was synthesized from 0.5–1.0 μg RNA using Superscript II Reverse Transcriptase (Invitrogen). Then, qRT-PCR was performed in triplicate with the ABI PRISM 7900HT sequence detection system (ABI) using SYBR green (Genecopoeia). Relative mRNA levels were calculated and normalized to 18S rRNA. The primers were used as follows: Sectm1a forward: 5'- ATGATGACCTGCCCTTCAGT GC, reverse: 5'- CTGGGTGTCTTT GATCACAAGC; 18S rRNA forward: 5'- GCAATTATTCCCC ATGAACG, reverse: 5'- GGCCTCACTAAACCATCCAA.

Lung histology and lung injury score

Lung tissues were collected from mice at 24 h post-CLP. All lungs were perfused *via* heart, inflated and fixed with 10% buffered formalin for more than two days, followed by embedded in paraffin, and cut into 5-μm sections. Tissue sections were stained with hematoxylin and eosin (H&E), examined with a light microscope (Olympus, Japan), and scored by a pathologist who was blinded to the experimental groups. To evaluate lung jury, 6–8 independent random lung fields were evaluated per mouse for neutrophils in alveolar spaces, neutrophils in the interstitial spaces, hyaline membranes, proteinaceous debris filling the airspaces, and alveolar septal thickening and weighted according to the relevance ascribed by the official American Thoracic Society workshop report on features and measurements of experimental acute lung injury in animals (22).

Measurement of cytokines and preparation of macrophages

Blood was collected at 18 h after CLP surgery and plasma samples were prepared by centrifuged at 3000 g for 15 min at 4°C. All plasmas were put into −80 °C until use. The concentration of cytokines was measured using Luminex Multiplex Immunoassay (Invitrogen) according to the manufacturer's protocol. For the isolation of peritoneal macrophages (PMs), 5 ml PBS was used to lavage the abdominal cavity of euthanized mice at 16 h post-CLP. The peritoneal lavage fluid was collected and centrifuged (1500 rpm, 5 mins). The cell pellet was then re-suspended in 5 ml fresh prepared DMEM media (10% FBS and 1% penicillin/streptomycin). Cells were allowed to adhere to the substrate by culturing them for 1–2 h at 37°C. Nonadherent cells were removed by gently washing three times with PBS. Mouse bone marrow-derived macrophages (BMDMs) were isolated as described previously (23) and cultured with 10% L929 media in DMEM complete media for

7 days. For the preparation of red pulp macrophages (RPMs) from spleen, mice were terminally anesthetized, and the spleen was carefully excised and thoroughly minced in PBS containing 3% FBS. The cell suspension was filtered through 70 μm Nylon cell strainer. Then, cells were pelleted by centrifuging 500 g for 5 min at 4°C. To lyse red blood cells (RBCs), cell pellets were suspended in RBC lysis buffer (Biolegend) for 4 min at room temperature (RT) and pelleted again. The resulting cell pellet was re-suspended in DMEM (Corning) containing 10% FBS, 10 mM HEPES and 1% penicillin/streptomycin solution (100 ×). Cells were seeded on 100 mm dish (5×10^7/well) or on the coverslip coated with collagen in 12-well plates (5×10^6/well). These cells were allowed to attach and grow for 7 days. Then, cells were washed with PBS for three times to dump these unattached cells, and culture medium was replaced by fresh one. After one day, cells were collected and used for following experiments.

Phagocytosis assay with *E. coli* bioparticles

To analyze the phagocytic capacity of PMs, BMDMs and RPMs isolated from WT and KO mice, cells were seeded onto 96-well plates (2.5×10^4 cells/well; or 5×10^4 cells/well) or on coverslips in 24-well plates (1×10^5 cells/well; or 2×10^5 cells/well) (DENVILLE, USA) in DMEM medium and allowed to adhere for 12 h. After treatment, pHrodo red E. coli bioparticles diluted in medium were added to wells according to the manuals. Subsequently, cells were incubated with bioparticles for 1 h at 37 °C. The fluorescence in the cell on 96-well plate was measured using a GloMax®-Multi Detection System (Promega). Cells cultured on coverslips were stained with CellMask™ Green Plasma Membrane Stain (Invitrogen) as described in the manual, then, fixed with 4% paraformaldehyde (10 min RT). After washing three times with PBS, coverslips were mounted onto slides using a ProLong diamond antifade mountant reagent with DAPI. Subsequently, slides were imaged with a confocal LSM 710 (Carl Zeiss Microimaging, Jena, Germany). Images were recorded with ZEN (Black) and analyzed with ImageJ software (Wayne Rasband, National Institutes of Health, Bethesda, MD).

Bacterial phagocytosis and killing assay

To determine bactericidal activity, a classical CFU (colony forming unit) assay was conducted with minor modifications as described previously (23). Briefly, *E. coli* DH5alpha were grown overnight in LB at 37°C. After that, bacteria were quantified, pelleted and washed with PBS. Then, bacteria were opsonized by incubation with diluted mice serum (20% serum in PBS) for 0.5 h at 37°C. BMDMs or RPMs were placed in 12-well culture plates with or without coverslips (2×10^5/well) and pre-incubated for 12 hours to allow to adhere. Subsequently, cells were treated with mouse IgG2a Fc (stoichiometrically matched to recombinant mouse Sectm1a-Fc), or recombinant mouse Sectm1a-Fc chimera protein (with Sectm1a fused to mouse IgG2a Fc; R&D Systems, Minneapolis, MN) for 20 h. Then, medium was exchanged with antibiotic-free fresh medium, and after 0.5 h, cells were infected with 2×10^6 CFU of live *E. coli*. After a 1 h incubation at 37°C with 5% CO_2, infected macrophages were washed two times with cold PBS, and fresh DMEM containing 100 μg/ml gentamicin was added to incubate for 30 min to kill extracellular bacteria. To determine internal bacteria at this time, cells were washed twice with PBS and lysed. The cell lysate was diluted serially and plated on the LB plate to determine the CFU count. To

assess the bactericidal activity, cells were incubated for another 4 h. The number of internalized bacteria was determined by lysing cell and plate the cell lysate as described in above. The killing percentage was calculated by using formula [(bacterial count at 1 h) - (bacterial count at 5 h) / (bacterial count at 1 h)] × 100.

Immunofluorescence staining

BMDMs were fixed on the coverslip, blocked with 1% BSA and incubated with primary antibody (DTA-1) diluted in 1% BSA overnight at 4°C. For rSectm1a blocking, BMDMs were incubated with rSectm1a for 12 h at 4°C before incubating with DTA-1. After washing, BMDMs were incubated with secondary antibody at room temperature for 1 h. Thereafter, cells were washed three times with PBS and mounted with ProLong diamond Antifade Mounting medium with DAPI (Invitrogen). Images were captured with Zeiss LSM710 LIVE Duo Confocal Microscope (Live Microscopy Core, University of Cincinnati).

Flow cytometry analysis

BMDMs were firstly blocked with CD16/32 antibody (clone 93) (eBioscience, 1:100 dilution) to prevent the non-specific binding to Fc receptors. Following blocking, part of BMDMs were incubated with rSectm1a before incubating with fluorescence-conjugated antibody. Following this, BMDMs were stained with PE-conjugated anti-mouse IgG2a (clone: RMG2a-62) or PE-Cy7-conjugated anti-mouse GITR (clone: DTA-1). RPMs isolated from spleen were also blocked with CD16/32 antibody (clone 93) (eBioscience, 1:100 dilution) to prevent the non-specific binding to Fc receptors. Following blocking, cells were stained with Pacific Blue-conjugated anti-mouse F4/80 (clone: BM8), PE-conjugated anti-mouse CD206 (clone: MMR), Alexa Fluor 750 conjugated anti-mouse SPIC (clone: Spi-1/PU.1).

Western blot analysis

Total protein was extracted from rSectm1a-treated BMDMs with or without *E. coli* bioparticles. Equal amounts of protein were subjected to SDS-PAGE and gel electrophoresis as described in previous study (24). Each membrane was stripped and re-probed with anti-GAPDH antibody for the detection of GAPDH as an internal loading control. Western blot bands were quantified by MultiImage II (AlphaInnotech, USA). The relative target protein levels were normalized to GAPDH. The following antibodies were used: rabbit anti-p-Akt (S473) (1:1000; Cell Signaling Technology); rabbit anti-Akt (1:1000; Cell Signaling Technology); rabbit anti-GAPDH (1:1000; Cell Signaling Technology).

Statistical Analysis

All data were tested for normality with Shapiro-Wilks test before statistical analysis. Statistical calculations were performed with GraphPad Prism 5.0 and all data were presented as mean ± SEM. Data were analyzed using 2-tailed Student's t test (normally distributed data) or Mann-Whitney test (non-normally distributed data) to determine the significance between population means when two groups were compared. For comparison of more than two groups, one-way ANOVA or two-way ANOVA were used to determine the significance. The survival rates were constructed using the Kaplan–Meier method, and differences in

mortality were compared using Log-rank (Mantel-Cox) test. A $p < 0.05$ was considered statistically significant.

Results

Loss of Sectm1a aggravates sepsis-induced multi-organ damage and mortality in mice

As mentioned above, Sectm1 was significantly lower in the blood of non-survivor sepsis patients compared to survivor controls (15). Yet, whether the expression of its homolog, Sectm1a, is altered in mice during polymicrobial sepsis remains unknown. To this end, we determined mRNA levels of Sectm1a in the blood, peritoneal macrophages, spleens and lungs of mice upon CLP surgery. As shown in Figure 1A-B, the expression level of Sectm1a in the blood was significantly reduced at 4 h post-CLP; whereas in peritoneal macrophages (PMs), Sectm1a expression was significantly down-regulated at later time point (18 h post-CLP). Remarkably, its most decrease (4.7-fold) was observed in the spleen at 4 h post-CLP (Fig. 1C). In addition, mRNA levels of Sectm1a in the spleen were still significantly decreased at 18 h post-CLP compared to sham controls (Fig. 1C). In the lung, Sectm1a expression was significantly down-regulated at 4 h and 18 h post-CLP. Taken together, these data suggest that reduction of Sectm1a may be related to the pathogenesis of polymicrobial sepsis. Given that Sectm1a is a secreted transmembrane protein, we therefore utilized CRISPR-CAS9 technology to generate a global Sectm1a-knockout (KO) mouse model (Fig. 1E, Supplement Fig. S1A) for exploring its possible role in sepsis condition. We validated the knock-out of Sectm1a by determining its expression with RT-PCR (Supplement Fig. S1B). Please note that we could not perform Western-blotting analysis to confirm, as Sectm1a antibody is not available now.

It is well known that spleen, the second largest lymphoid organ, plays important roles in immunity (25). Loss of splenic function, either by splenectomy or infiltrative disease, prominently increases the risk for severe infection and sepsis (26). Considering that Sectm1a is highly expressed in the spleen (18), we firstly determined whether loss of Sectm1a augmented splenomegaly (or spleen edema) in mice during polymicrobial sepsis. As indicated in Figure 1F, KO-spleens displayed remarkably higher ratio of wet/dry weight than WT controls after CLP surgery, implicating aggravated edema caused by the loss of Sectm1a. Next, we assessed lung injury in WT and Sectm1a-KO mice at the same time point. Similar effects and trends were observed in the wet/dry weight ratio of the lung (Fig. 1G). Meanwhile, we examined lung histology (Fig. 1H) and observed that lung tissues collected from CLP-treated KO mice presented extensive morphological damage and pathologic abnormalities (injury score: 0.49), compared to that in CLP-treated WT mice (injury score: 0.39, Fig. 1I), evidenced by: 1) the infiltration of neutrophils into interstitial and alveolar spaces, 2) increased hyaline membranes, and 3) increased alveolar wall thickness and alveolar collapse (Fig. 1H). Accordingly, CLP-KO mice exhibited 40% higher mortality rate with median survival of 30 h, compared to CLP-WT mice (median survival: 70 h, n = 10–12) (Fig. 1J). Put together, these data indicate that loss of Sectm1a significantly exacerbates CLP-induced organ damage and mortality in mice.

Lack of Sectm1a augments systemic inflammation and bacterial burden in CLP-mice

Given that multi-organ failure in sepsis is ascribe to uncontrolled bacterial proliferation and dissemination as well as the excessive release of pro-inflammatory cytokines (27), we next determined systemic inflammation and bacterial clearance in both WT and KO mice after CLP surgery. Interestingly, we observed that cytokines, such as IL-1β, IL-6, IL-10, and TNF-α, were significantly elevated in the blood of Sectm1a-KO mice at 12 hours post-CLP, when compared to WT-samples (Fig. 2A-D). Notably, Sectm1a deficiency did not alter basal levels of these cytokines (Fig. 2A-D). More importantly, MCP-1, as a predictive marker for sepsis prognosis (28, 29), was dramatically increased by 3.6-fold in sera of Sectm1a-KO mice compared to that in WT mice after CLP (Fig. 2E). Considering that MCP-1 is one of the key chemokines that regulate monocyte/macrophage migration (30), its elevation in the blood of Sectm1a-KO mice may contribute to the infiltration of monocytes/macrophages into organs. This is in line with our above results that loss of Sectm1a caused organ damage to a greater degree and higher mortality in response to CLP surgery (Fig. 1 F-J).

In addition, the presence of bacteria was examined in the peritoneal lavage, blood, spleen and lung of WT and Sectm1a-KO mice at 12 h post-CLP. We found that levels of bacteria detected in the peritoneal lavage and blood were markedly higher in CLP-treated KO mice than those in CLP-WT mice (Fig. 2F and G). Likewise, bacterial loads in lungs and spleens were also significantly elevated by Sectm1a depletion (Fig. 2H and I). These results indicate that Sectm1a might be an important regulator in controlling bacterial dissemination during sepsis.

Depletion of Sectm1a impairs phagocytic and bactericidal activities of macrophages

To further examine the effect of Sectm1a on the control of bacterial dissemination, we next conducted bacterial phagocytosis and intracellular killing assays in peritoneal macrophages (PMs), bone-marrow-derived macrophages (BMDMs), and red pulp macrophages (RPMs) isolated from WT and Sectm1a-KO mice. The uptake of red fluorescence-conjugated *E. coli* bioparticles were assessed in peritoneal macrophages (PMs) by fluorescent microscopy (Fig. 3A) and quantified with Image J (Fig. 3B). Our results showed that the average of red fluorescence intensity in KO-PMs was significantly lower than that in WT-PMs (Fig. 3A and B), indicating that Sectm1a deficiency significantly decreases phagocytic activity of peritoneal macrophages. In addition, when using live *E. coli* to infect BMDMs, we found that the loss of Sectm1a not only significantly reduced bacterial uptake by 30% (Fig. 3C) but also remarkably decreased intracellular killing activity by 27% in BMDMs (Fig. 3D). To validate these results, we further analyzed phagocytic activity of BMDMs using red fluorescence-conjugated *E. coli* bioparticles (Fig. 3E-G) and revealed that KO-BMDMs had significant lower phagocytic activity, compared to WT-BMDMs. Furthermore, considering that RPMs, as tissue-resident macrophages in the spleen (31), play important roles not only in scavenging senescent erythrocytes but also in controlling bacteria-caused infection through recognizing and eliminating bacteria from circulation (32), we therefore compared phagocytic and bactericidal activities between WT-RPMs and KO-RPMs. The purity of isolated RPMs was determined by flow cytometry analysis of macrophage membrane markers (F4/80, CD206 and SPIC, Supplemental Fig. S2A-B), and confirmed by immunofluorescence staining with F4/80 (Supplemental Fig. S2C). As expected, loss of

Sectm1a dramatically impaired phagocytosis and bacterial clearance abilities of RPMs (Fig. 3H and I). Collectively, these data suggest that the absence of Sectm1a significantly impairs bacterial clearance in both recruited macrophages and tissue-resident macrophages, leading to increased bacterial burden in mice during sepsis.

rSectm1a enhances phagocytosis and bactericidal capacity of macrophages

Given that Sectm1a can be secreted into the extracellular environment (17, 18), we next aimed to investigate the effect of recombinant Sectm1a protein (rSectm1a) on phagocytic and bactericidal activities of macrophages. Since rSectm1a is a recombinant mouse Sectm1a-Fc chimera protein (with Sectm1a fused to mouse IgG2a), we used stoichiometrically matched amount of mouse IgG2a as isotype control. After stimulating with rSectm1a or control IgG2a for 20 h, the bacterial uptake and clearance activity of WT-BMDMs were assessed by incubating with live *E. coli*. The rSectm1a-treated WT-BMDMs showed a significant increase in bacterial phagocytosis and killing rate compared with IgG2a-treated WT-BMDMs (Fig. 4A and B). This elevation in phagocytosis was further confirmed by using red fluorescence-conjugated *E. coli* bioparticles and showed that treatment of WT-BMDMs with rSectm1a remarkably increased uptake of *E. coli* bioparticles by 40% (Fig. 4C). In addition, rSectm1a could improve bacterial uptake and clearance activity in KO-BMDMs (Fig. 4D-G). Furthermore, RPMs stimulated with rSectm1a showed 20% increase in bacterial uptake (Fig. 4H) and 2-fold increase in bacterial killing (Fig. 4I), compared to the isotype controls. Such results were further confirmed using *E. coli* bioparticles in RPMs (Fig. 4J and K). Taken together, our data suggest that rSectm1a could enhance defense function of both recruited and tissue-resident macrophages in response to bacterial infection.

Therapeutic effects of rSectm1a in WT mice upon CLP surgery

To further determine whether rSectm1a had any therapeutic effects *in vivo* against polymicrobial sepsis, we injected WT mice with a single dose of rSectm1a (300 μg/kg, *i.v.*) or control IgG2a at 0.5 h post-CLP surgery. We observed that administration of septic mice with rSectm1a significantly improved survival outcome, as evidenced by 75% of rSectm1a-treated mice (n = 8) survived at 96 h post-CLP, when only 33.3% of IgG2a-treated mice survived (n = 15) (Fig. 5A). In line with the survival data, the ratios of wet/dry weight in spleens (Fig. 5B) and lungs (Fig. 5C) collected from rSectm1a-treated CLP-mice were significantly lower than those samples from IgG2a-treated CLP-mice. In addition, administration of rSectm1a into CLP-mice significantly reduced bacterial burdens in the blood (Fig. 5D), spleen (Fig. 5E) and lung (Fig. 5F) to a greater degree, compared to IgG2a-treated control mice. Lastly, the serum levels of pro-inflammatory cytokines (*i.e.*, IL-6 and TNF-α) in rSectm1a-treated CLP-mice were also significantly decreased, compared to IgG2a-treated control mice (Fig. 5G and H). Collectively, these data indicate that administration of rSectm1a could improve animal survival, attenuate organ injury, increase bacterial clearance and reduce systemic inflammatory response in CLP-induced septic mice.

rSectm1a promotes macrophage bacterial clearance through activation of GITR

GITR, also known as TNFRS18, is expressed in various cell types of the immune system including macrophages (33). Recently, Howie *et al* identified GITR as a potential Sectm1a-

binding partner in T cells (18). However, it remains unclear whether Sectm1a could bind GITR on the surface of macrophages and activate its downstream signaling pathway. To exclude the endogenous Sectm1a, we utilized BMDMs that were isolated from Sectm1a-KO mice and incubated with rSectm1a protein after blocking with 1% BSA. Then, we washed with PBS and incubated with red fluorescence-conjugated secondary antibody (anti-mouse IgG2a) to detect whether rSectm1a directly bound to cell surface [Note: rSectm1a protein contains an immunoglobulin FC domain (IgG2a)]. As shown in Figure 6A, strong red fluorescence was remained on the membrane of KO-BMDMs, implicating that rSectm1a protein was able to bind to macrophages. Next, after blocking, we incubated KO-BMDMs with IgG2a or rSectm1a, followed by staining GITR with its antibody DTA-1 to determine whether rSectm1a competed with DTA-1 to bind GITR. Remarkably, BMDMs incubated with control IgG2a showed no interference on the binding of DTA-1 to its receptor, GITR (Fig. 6B, green dots). However, DTA-1 could not bind to GITR on the surface of rSectm1a-pretreated BMDMs, as evidenced by virtually no green-dot staining signal of DTA-1(Fig. 6B). These results indicate that rSectm1a competes with DTA-1 for the binding to GITR. To further validate these findings, we performed Flow Cytometry analysis (FCAS) in KO-BMDMs after incubating with different concentrations of rSectm1a and observed that higher concentration (2μg/ml) resulted in higher amount of red fluorescence signal on the surface of BMDMs (Fig. 6C). In addition, using the similar design strategy as Figure 6B, our flow cytometry confirmed that pre-incubating BMDMs with rSectm1a successfully blocked binding of DTA-1 to GITR (Fig. 6D). Hence, both immuno-staining and FACS results consistently suggest that Sectm1a could interact with GITR on the surface of macrophages.

To elucidate the role of GITR in macrophage phagocytosis of bacteria, we stimulated BMDMs with DTA-1 for phagocytosis assay. As shown in Figure 6, E-G, treatment of BMDMs with DTA-1 significantly increased bacterial uptake and clearance, compared to the isotype controls. This indicates that the activation of GITR promotes bactericidal activities of macrophages. To further determine whether GITR is essential for Sectm1a-mediated phagocytosis, we isolated BMDMs from GITR-knockout mice and conducted phagocytosis and intracellular killing assay. Interestingly, pre-treatment of GITR-KO BMDMs with rSectm1a did not improve bacterial phagocytosis and clearance, when compared to IgG2a control (Fig. 6H-J). Lastly, we injected rSectm1a into GITR-KO mice at 0.5 h post CLP surgery and observed that, unlike its beneficial effects in WT-mice (Fig. 5A), administration of rSectm1a did not attenuate CLP-induced mortality in GITR-KO mice (Fig. 6K). Put together, these data indicate that rSectm1a-elicited improvement in the outcome of polymicrobial sepsis is largely ascribed to its interaction with GITR in macrophages.

Pharmacologically inhibition of PI3K-Akt pathway abolishes the effects of rSectm1a on macrophage function

Given that the activation of GITR is a potential trigger of phosphoinositide 3-kinase (PI3K)-Akt pathway in T lymphocytes (34), we speculated that Sectm1a may activate PI3K-Akt pathway in macrophages through binging to GITR. Therefore, we examined Akt phosphorylation in BMDMs with or without rSectm1a pretreatment. Our Western-blotting analysis results showed that BMDMs pre-stimulated with rSectm1a displayed ~1.5-fold increase in the levels of phosphorylated Akt, compared to that in isotype-controls (Fig. 7A

and B). Importantly, challenge of BMDMs with *E. coli* Bioparticles also activated Akt, which was more pronounced in rSectm1a-treated BMDMs than that in IgG2a-treated controls (Fig. 7A and B). To investigate whether Sectm1a-induced bacterial phagocytosis and killing by macrophage is dependent on the activation of PI3K-Akt pathway, we pre-treated BMDMs with LY294002 or wortmannin (WM), specific inhibitors of the PI3K signaling pathway, before stimulating with rSectm1a. The phagocytosis analysis results showed that pre-inhibition of PI3K in macrophages by LY294002 completely abolished rSectm1a-induced bacterial entry, as evidenced by no any differences in the bioparticle-fluorescence intensity (Fig. 7C) and live *E. coli* colony count (Fig. 7D) between rSectm1a- and IgG2a-treated BMBMs. Accordingly, rSectm1a-induced bacterial killing capacity in BMDMs was also blocked by pre-treatment with LY294002 (Fig. 7E). These results were further confirmed in BMDMs using another PI3K inhibitor, wortmannin (WM) (Fig. 7F-H). Interestingly, similar findings were observed in spleen residential macrophages (RPMs) (Fig. 7I-K). Taken together, these data indicate that Sectm1a-mediated bacterial clearance in macrophages may rely on the activation of PI3K-Akt pathway.

Discussion

It is well recognized that the impaired macrophage phagocytosis and intracellular killing of bacteria is primarily responsible for the insufficient antibacterial defense and hyper-inflammation in severe septic patients (12, 35). In this study, we define that Sectm1a, as a novel GITR ligand, plays a critical role in regulating macrophage function against bacterial infection. We found that loss of Sectm1a augmented CLP-induced bacterial dissemination, systemic inflammation, multiple organ injury and animal mortality. Importantly, we revealed that Sectm1a depletion impaired bactericidal activities in both recruited and tissue-resident macrophages. By contrast, addition of rSectm1a to macrophages significantly promoted bacterial uptake and clearance. The mechanical study showed that Sectm1a was able to bind to GITR on the surface of macrophages and activated PI3K-Akt pathway, leading to enhanced phagocytic activity of macrophages and improved survival outcomes of septic mice.

As fundamental components of innate immunity, macrophages are the most abundant immune cells in many tissues and play critical roles throughout all phases of sepsis (35). Previous dogma suggested that all macrophages were terminally differentiated immune cells derived from circulating monocytes (bone marrow origin) (36). Therefore, most studies about bacterial defense function of macrophages focused on bone marrow-derived macrophages (BMDMs). However, recent evidence showed that most macrophages residing in the organ, referred to as tissue-resident macrophages, are originated from embryonic progenitors, persist into adulthood, and self-maintained by local proliferation rather than monocyte recruitment (36, 37). Although tissue-resident macrophages share some similar functions (i.e., scavenging invading pathogens) with recruited BMDMs (38), studies on the bacterial defense function of tissue-resident macrophages have been limited so far. For example, RPMs, as tissue-resident macrophages in the spleen, were recently proved to play an essential role in eliminating bacteria from circulation and contributed to suppressing bacteria dissemination (31, 38). However, it remains unclear regarding the regulatory mechanism behind the bacterial clearance activity of RPMs. In the present study, we identify

Sectm1a as a novel positive regulator for the bacterial defense function in both recruited macrophages (BMDMs) and tissue-resident macrophages (*i.e.,* RPMs).

Glucocorticoid-induced tumor necrosis factor (TNF) receptor family-related protein ligand (GITRL) is mainly expressed on macrophages, dendritic cells, endothelial cells, and B cells (39). Its cognate receptor, GITR, was initially detected in various T-cell types such as naive T cells, $CD4^+$ $CD25^+$ regulatory T cells, and activated $CD25^-$ effector T cells (40). However, several recent studies have demonstrated that GITR is also expressed on macrophages (41–44). So far, the function of GITRL has been intensively studied as a co-stimulator molecule that interacts with GITR on T cell membrane (45). In comparison, less efforts have been made toward understanding the effects of GITRL/GITR interaction on macrophage function. Some *in vitro* studies showed that GITRL stimulation caused an increase in cytokine release and cellular aggregation in macrophage cell line (THP-1) (41, 42) as well as inflammatory gene expression in microglial cell line (43). Notably, a recent *in vitro* study by Fu *et al.* showed that GITRL accelerated migration and promoted phagocytosis and killing function of macrophages (RAW264.7 and THP-1) (44). Consistently, we observed in the present study that Sectm1a, as a novel autocrine and paracrine GITRL, promoted macrophage phagocytosis and killing capacity of bacteria; whereas global knockout of Sectm1a resulted in a significant increase in bacterial dissemination, systemic inflammation and animal mortality during polymicrobial sepsis induced by CLP surgery. Giving that antibiotic therapy is a basic clinical treatment of sepsis, the major limitation in the present study is that we did not give antibiotics to CLP mice to mimic the clinic condition for the treatment of sepsis patients. In addition, with respect to the *in vitro* bacterial killing assays, we could not treat macrophages with rSectm1a after these cells have phagocytosed the bacteria to disentangle phagocytosis and killing, like previous work done by Csóka *et al* (46). The reason is that Sectm1a-mediated effects on macrophage phagocytosis and killing of bacteria are largely dependent on the activation of GITR, which may take longer time (39, 43). Indeed, previous works has reported that stimulation of GITR in macrophages is observed after overnight or 24 h treatment with ligands (39, 43). Likewise, in the present study, we pretreated macrophages with rSectm1a for 20 h to activate GITR, followed by phagocytosis and killing assays. Furthermore, in this study we showed that Sectm1a deficiency led to decreased bacterial killing, which was conducted by comparing the viable bacterial colony counts within macrophages at different time points, and results were calculated using the formula: [(bacterial count at 1 h) - (bacterial count at 5 h) / (bacterial count at 1 h)] × 100. Therefore, results from this assay will not be confounded by the difference on phagocytosis activity.

Currently, it is well appreciated that activation of PI3K-Akt is a common response triggered by a range of membrane-bound receptors such as toll-like receptors, cytokine receptors and tumor necrosis factor receptor super family molecules (TNFRSFs) (34). Among these TNFRSFs, GITR is able to provide costimulatory signals similar as CD28 ligation to activate PI3K-Akt pathway in T cells (34). In the present study, we identified that Sectm1a physically interacted with GITR on the surface of macrophages, and rSectm1a-treated BMDMs showed higher levels of phosphorylated Akt compared to control IgG2a-treated macrophages. This suggests that the interaction between Sectm1a and GITR could activate PI3K-Akt pathway in macrophages. Interestingly, recent studies have demonstrated that the

activation of PI3K-Akt pathway is critical in up-regulating bacterial phagocytosis and intracellular killing activity (47, 48). Consistently, in the present study, we discovered that pharmacologically inhibition of the PI3K-Akt pathway in macrophages completely abolished rSectm1a-mediated bacteria defense function in macrophages, indicating that rSectm1a-induced bacterial uptake and clearance might be dependent on the activation of PI3K-Akt pathway. Furthermore, the PI3K-Akt signaling pathway has been shown to play a significant role in the establishment of endotoxin tolerance in macrophages and restricting proinflammatory response in macrophages (47). Hence, these previous findings, at least, partially explains the remarkable increase of pro-inflammatory cytokines in the plasma of Sectm1a-KO mouse compared with those in WT mice.

The effective and timely immune response to infection is optimal for the host defense by avoiding the consequences of excessive inflammation during sepsis. Our data presented in this study demonstrate that Sectm1a, as a novel autocrine and paracrine GITRL, positively regulates phagocytic and bactericidal function of macrophages through activating PI3K-Akt pathway. Down-regulation or depletion of Sectm1a would augment bacterial dissemination, promote inflammatory cytokine production, exaggerate organ damages, and increase animal mortality. Thus, these preclinical data in CLP-mouse model may provide the proof of principle for a novel approach to improve survival during sepsis through interventions targeting Sectm1 in human patients.

Supplementary Material

Refer to Web version on PubMed Central for supplementary material.

3. Financial support

This study was supported by National Institutes of Health (NIH) grants R01 GM-126061, R01 GM-132149, and American Heart Association (AHA) Established Investigator Award 17EIA33400063 (G.-C. Fan).

References

1. Fleischmann C, Scherag A, Adhikari NK, Hartog CS, Tsaganos T, Schlattmann P, Angus DC, and Reinhart K 2016 Assessment of Global Incidence and Mortality of Hospital-treated Sepsis. Current Estimates and Limitations. Am. J. Respir. Crit. Care Med. 193: 259–272. [PubMed: 26414292]
2. Paoli CJ, Reynolds MA, Sinha M, Gitlin M, and Crouser E 2018 Epidemiology and Costs of Sepsis in the United States-An Analysis Based on Timing of Diagnosis and Severity Level. Crit. Care Med. 46: 1889–1897. [PubMed: 30048332]
3. Gaieski DF, Edwards JM, Kallan MJ, and Carr BG 2013 Benchmarking the incidence and mortality of severe sepsis in the United States. Crit, Care Med. 41: 1167–1174. [PubMed: 23442987]
4. Hershey TB, and Kahn JM 2017 State Sepsis Mandates-A New Era for Regulation of Hospital Quality. N. Engl. J. Med. 376: 2311–2313. [PubMed: 28528558]
5. Angus DC, Mira JP, and Vincent JL 2010 Improving clinical trials in the critically ill. Crit. Care Med. 38: 527–532. [PubMed: 19851096]
6. Osuchowski MF, Craciun F, Weixelbaumer KM, Duffy ER, and Remick DG 2012 Sepsis chronically in MARS: systemic cytokine responses are always mixed regardless of the outcome, magnitude, or phase of sepsis. J. Immunol. 189: 4648–4656. [PubMed: 23008446]
7. Tosi M, Roat E, De Biasi S, Munari E, Venturelli S, Coloretti I, Biagioni E, Cossarizza A, and Girardis M 2018 Multidrug resistant bacteria in critically ill patients: a step further antibiotic therapy. J. Emerg. Crit. Care Med. 2: 1–9.

8. Andrews T, and Sullivan KE 2003 Infections in patients with inherited defects in phagocytic function. Clin. Microbiol. Rev 16: 597–621. [PubMed: 14557288]

9. Danikas DD, Karakantza M, Theodorou GL, Sakellaropoulos GC, and Gogos CA 2008 Prognostic value of phagocytic activity of neutrophils and monocytes in sepsis. Correlation to CD64 and CD14 antigen expression. Clin. Exp. Immunol 154: 87–97. [PubMed: 18727624]

10. Rydell-Törmänen K, Uller L, and Erjefält JS 2006 Neutrophil cannibalism–a backup when the macrophage clearance system is insufficient. Respir. Res. 7: 143. [PubMed: 17166290]

11. Uderhardt S, Martins AJ, Tsang JS, Lämmermann T, and Germain RN 2019 Resident macrophages cloak tissue microlesions to prevent neutrophil-driven inflammatory damage. Cell 177: 541–555. [PubMed: 30955887]

12. Hotchkiss RS, Monneret G, and Payen D 2013 Immunosuppression in sepsis: a novel understanding of the disorder and a new therapeutic approach. Lancet Infect. Dis. 13: 260–268. [PubMed: 23427891]

13. Lyman SD, Escobar S, Rousseau AM, Armstrong A, and Fanslow WC 2000 Identification of CD7 as a cognate of the human K12 (SECTM1) protein. J. Biol. Chem. 275: 3431–3437. [PubMed: 10652336]

14. Wang T, Huang C, Lopez-Coral A, Slentz-Kesler KA, Xiao M, Wherry EJ, and Kaufman RE 2012 K12/SECTM1, an interferon-γ regulated molecule, synergizes with CD28 to costimulate human T cell proliferation. J. Leukoc. Biol. 91: 449–459. [PubMed: 22184754]

15. Tsalik EL, Langley RJ, Dinwiddie DL, Miller NA, Yoo B, van Velkinburgh JC, Smith LD, Thiffault I, Jaehne AK, Valente AM, et al. 2014 An integrated transcriptome and expressed variant analysis of sepsis survival and death. Genome Med. 6: 111. [PubMed: 25538794]

16. Mu X, Li Y, Fan H, Essandoh K, Deng S, Wang X, Wang P, Wang L, Fan GC 2019 Sectm1a positively regulates tissue-resident macrophage self-renewal capacity during endotoxemia by boosting T effector cells. Shock 51: 57.

17. Kamata H, Yamamoto K, Wasserman GA, Zabinski MC, Yuen CK, Lung WY, Gower AC, Belkina AC, Ramirez MI, Deng JC, et al. 2016 Epithelial cell–derived secreted and transmembrane 1a signals to activated neutrophils during pneumococcal pneumonia. Am. J. Respir. Cell Mol. Biol. 55: 407–418. [PubMed: 27064756]

18. Howie D, Rueda HG, Brown MH, and Waldmann H 2013 Secreted and transmembrane 1A is a novel co-stimulatory ligand. PloS One 8: e73610. [PubMed: 24039998]

19. Li Y, Deng S, Wang X, Huang W, Chen J, Robbins N, Mu X, Essandoh K, Peng T, Jegga AG, et al. 2020 Sectm1a deficiency aggravates inflammation-triggered cardiac dysfunction through disruption of LXRα signaling in macrophages. Cardiovasc Res. Mar 14: cvaa067. doi:10.1093/cvr/cvaa067.

20. Toscano MG, Ganea D, and Gamero AM 2011 Cecal ligation puncture procedure. JoVE. 51: e2860.

21. Jin L, Batra S, and Jeyaseelan S 2017 Deletion of Nlrp3 augments survival during polymicrobial sepsis by decreasing autophagy and enhancing phagocytosis. J. Immunol. 198: 1253–1262. [PubMed: 28031338]

22. Matute-Bello G, Downey G, Moore BB, Groshong SD, Matthay MA, Slutsky AS, and Kuebler WM 2011 An official American Thoracic Society workshop report: features and measurements of experimental acute lung injury in animals. Am. J. Respir. Cell Mol. Biol. 44: 725–738. [PubMed: 21531958]

23. Bai F, McCormack RM, Hower S, Plano GV, Lichtenheld MG, and Munson GP 2018 Perforin-2 breaches the envelope of phagocytosed bacteria allowing antimicrobial effectors access to intracellular targets. J. Immunol. 201: 2710–2720. [PubMed: 30249808]

24. Mu X, Wang X, Huang W, Wang RT, Essandoh K, Li Y, Pugh AM, Peng J, Deng S, Wang Y, et al. 2018 Circulating exosomes isolated from septic mice induce cardiovascular hyperpermeability through promoting podosome cluster formation. Shock 49: 429–441. [PubMed: 28650928]

25. Bronte V, and Pittet MJ 2013 The spleen in local and systemic regulation of immunity. Immunity 39: 806–818. [PubMed: 24238338]

26. Edgren G, Almqvist R, Hartman M, and Utter GH 2014 Splenectomy and the risk of sepsis: a population-based cohort study. Ann. Surg. 260: 1081–1087. [PubMed: 24374533]

27. Cohen J 2002 The immunopathogenesis of sepsis. Nature 420: 885–891. [PubMed: 12490963]
28. Osuchowski MF, Welch K, Siddiqui J, and Remick DG 2006 Circulating cytokine/inhibitor profiles reshape the understanding of the SIRS/CARS continuum in sepsis and predict mortality. J. Immunol. 177: 1967–1974. [PubMed: 16849510]
29. Zhu T, Liao X, Feng T, Wu Q, Zhang J, Cao X, and Li H 2017 Plasma monocyte chemoattractant protein 1 as a predictive marker for sepsis prognosis: a prospective cohort study. Tohoku J. Exp. Med. 241: 139–147. [PubMed: 28202856]
30. Deshmane SL, Kremlev S, Amini S, and Sawaya BE 2009 Monocyte chemoattractant protein-1 (MCP-1): an overview. J. Interferon Cytokine Res. 29: 313–326. [PubMed: 19441883]
31. Mu X, Li Y, Fan G-C 2020. Tissue-resident macrophages in the control of infection and resolution of inflammation. Shock. doi: 10.1097/SHK.0000000000001601.
32. Borges da Silva H, Fonseca R, Pereira RM, Cassado ADA, Álvarez JM, and D'Império Lima MR 2015 Splenic macrophage subsets and their function during blood-borne infections. Front. Immunol. 6: 480. [PubMed: 26441984]
33. Kim WJ, Bae EM, Kang YJ, Bae HU, Hong SH, Lee JY, Park JE, Kwon BS, Suk K, and Lee WH 2006 Glucocorticoid-induced tumor necrosis factor receptor family related protein (GITR) mediates inflammatory activation of macrophages that can destabilize atherosclerotic plaques. Immunology 119: 421–429. [PubMed: 17067317]
34. So T, and Croft M 2013 Regulation of PI-3-kinase and Akt signaling in T lymphocytes and other cells by TNFR family molecules. Front. Immunol. 4: 139. [PubMed: 23760533]
35. Hotchkiss RS, Moldawer LL, Opal SM, Reinhart K, Turnbull IR, and Vincent JL 2016 Sepsis and septic shock. Nat. Rev. Dis. Primers 2: 1–21.
36. Sieweke MH and Allen JE 2013 Beyond stem cells: self-renewal of differentiated macrophages. Science 342: 1242974. [PubMed: 24264994]
37. Hashimoto D, Chow A, Noizat C, Teo P, Beasley MB, Leboeuf M, Becker CD, See P, Price J, Lucas D, et al. 2013Tissue-resident macrophages self-maintain locally throughout adult life with minimal contribution from circulating monocytes. Immunity 38: 792–804. [PubMed: 23601688]
38. Epelman S, Lavine KJ, and Randolph GJ 2014 Origin and functions of tissue macrophages. Immunity. 41: 21–35. [PubMed: 25035951]
39. Kim JI, Sonawane SB, Lee MK, Lee SH, Duff PE, Moore DJ, O'Connor MR, Lian MM, Deng S, Choi Y, et al. 2010 Blockade of GITR–GITRL interaction maintains Treg function to prolong allograft survival. Eur. J. Immunol. 40: 1369–1374. [PubMed: 20148423]
40. MacHugh RS, Piccirilo C, Young DA, Shevach EM, Collins M, and Byrne C 2002 CD4 (+) CD25 (+) immunoregulatory T cells: gene expression analysis reveals a functional role for the glucocorticoid-induced TNF receptor. Immunity 16: 311–323. [PubMed: 11869690]
41. Bae E, Kim WJ, Kang YM, Suk K, Koh EM, Cha HS, Ahn KS, Huh TL, and Lee WH 2007 Glucocorticoid-induced tumour necrosis factor receptor-related protein-mediated macrophage stimulation may induce cellular adhesion and cytokine expression in rheumatoid arthritis. Clin. Exp. Immunol. 148: 410–418. [PubMed: 17359498]
42. Bae EM, Kim WJ, Suk K, Kang YM, Park JE, Kim WY, Choi EM, Choi BK, Kwon BS, and Lee WH 2008 Reverse signaling initiated from GITRL induces NF-κB activation through ERK in the inflammatory activation of macrophages. Mol. Immunol. 45: 523–533. [PubMed: 17602748]
43. Hwang H, Lee S, Lee WH, Lee HJ, and Suk K 2010 Stimulation of glucocorticoid-induced tumor necrosis factor receptor family-related protein ligand (GITRL) induces inflammatory activation of microglia in culture. J. Neurosci. Res. 88: 2188–2196. [PubMed: 20162721]
44. Fu Z, Wang S, Li J, Zhang Y, Li H, Li G, Wan X, and Zhang Y 2020. Biological role of GITR/GITRL in attributes and immune responses of macrophage. J. Leukoc. Biol. 107: 309–321. [PubMed: 31833599]
45. Kanamaru F, Youngnak P, Hashiguchi M, Nishioka T, Takahashi T, Sakaguchi S, Ishikawa I, and Azuma M 2004 Costimulation via glucocorticoid-induced TNF receptor in both conventional and $CD25^+$ regulatory $CD4^+$ T cells. J. Immunol. 172:7306–7314. [PubMed: 15187106]
46. Csóka B, Németh ZH, Szabó I, Davies DL, Varga ZV, Pálóczi J, Falzoni S, Di Virgilio F, Muramatsu R, Yamashita T, et al. 2018 Macrophage P2X4 receptors augment bacterial killing and protect against sepsis. JCI insight 3: e99431.

47. Vergadi E, Ieronymaki E, Lyroni K, Vaporidi K, and Tsatsanis C 2017 Akt signaling pathway in macrophage activation and M1/M2 polarization. J. Immunol. 198: 1006–1014. [PubMed: 28115590]

48. Wang S, Deng S, Cao Y, Zhang R, Wang Z, Jiang X, Wang J, Zhang X, Zhang J, Liu G, et al. 2018 Overexpression of toll-like receptor 4 contributes to phagocytosis of salmonella enterica serovar typhimurium via phosphoinositide 3-kinase signaling in sheep. Cell Physiol. Biochem. 49: 662–677. [PubMed: 30165358]

Key points

1. Sectm1a enhances macrophage clearance of bacteria through activating GITR
2. Sectm1a deficiency worsens the outcome of polymicrobial sepsis

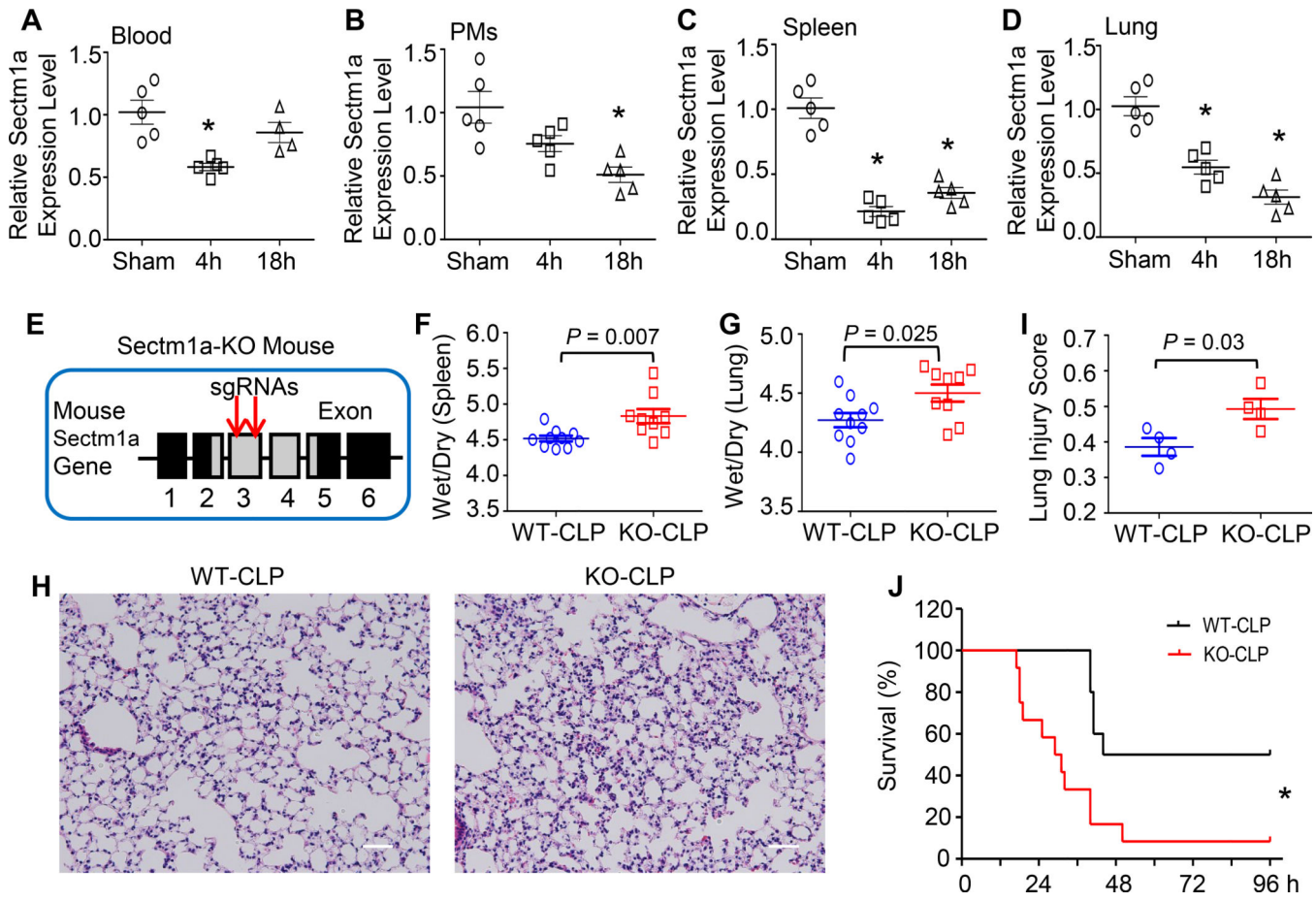

Figure 1. Sectm1a depletion aggravates polymicrobial sepsis-induced multi-organ damage and mortality.

(A-D) Expression levels of Sectm1a were determined in (A) blood, (B) peritoneal macrophages (PMs), (C) spleen and (D) lung collected from WT mice at indicated time points after CLP surgery (*, $P < 0.05$; n = 5). (E) Two gRNAs targeting to Exon3 of Sectm1a gene were selected to generate Sectm1a-KO mouse model, detailed in Ref. 19. (F-G) At 24 h post-CLP, wet weight to dry weight ratios of spleen (F) and lung (G) were quantified (n = 9–10). (H) Representative images of lung section with H&E staining at 24 h after CLP surgery were shown at ×200 original magnification. Scale bars, 50 μm. (I) Lung injury scores were assessed as described in Materials and Methods (n = 4). (J) WT (n=10) and Sectm1a-KO mice (n=12) were monitored for survival up to 96 h after CLP surgery and analyzed by Log-rank (Mantel-Cox) test. Data are representative of two (A-D, H-J) or three (F-G) independent experiments. Except survival test, all other results are presented as mean ± SEM and analyzed by one-way ANOVA or student's t test.

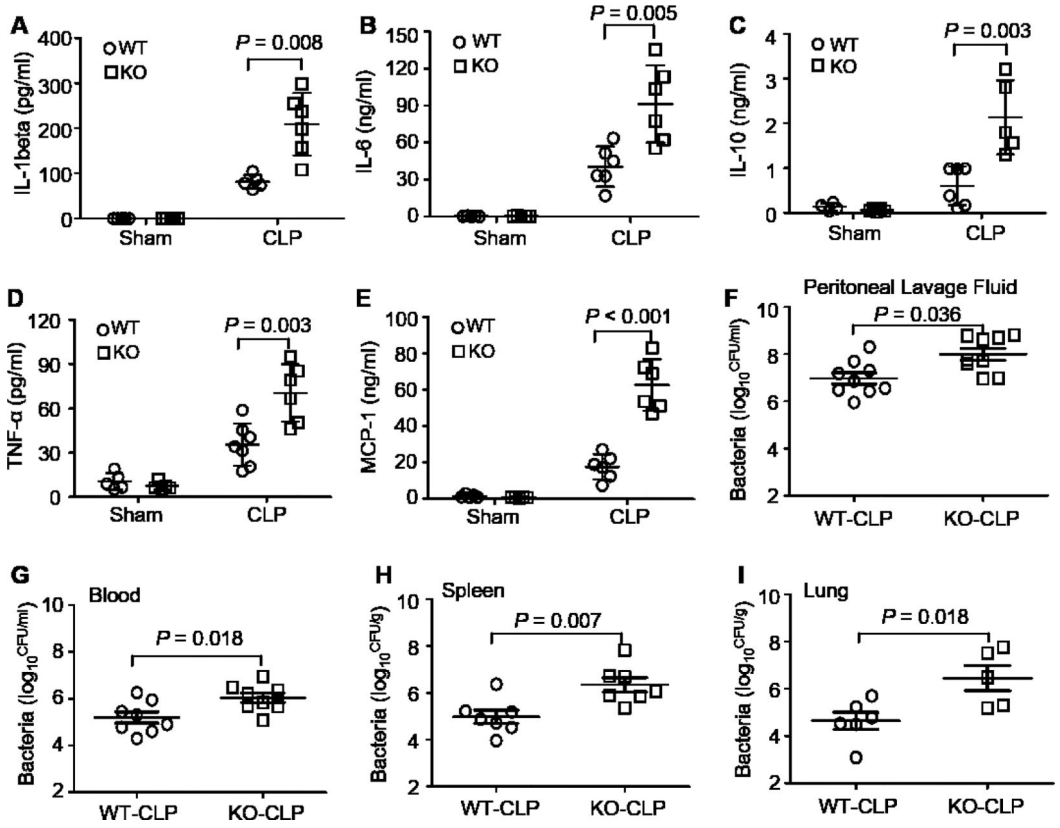

Figure 2. Sectm1a deficiency enhances systemic inflammation and bacterial burden.

(A-E) Serum levels of cytokines (A: IL-1β; B: IL-6; C: IL-10; D: TNF-α; E: MCP-1) were measured in WT and Sectm1a-KO mice at 12 h after CLP surgery (n = 5–7). (F-G) Bacterial burdens in both peritoneal lavage fluid (F) and blood (G) were compared between WT mice and Sectm1a-KO mice at 18 h post-CLP operation (n = 8). (H-I) At 24 h post-CLP surgery, spleen and lung were collected from WT mice and Sectm1a-KO mice, and bacterial burdens in these tissues were compared between two models (n = 5–7). Data are representative of two independent experiments. All results are presented as mean ± SEM and analyzed by student's t test or two-way ANOVA.

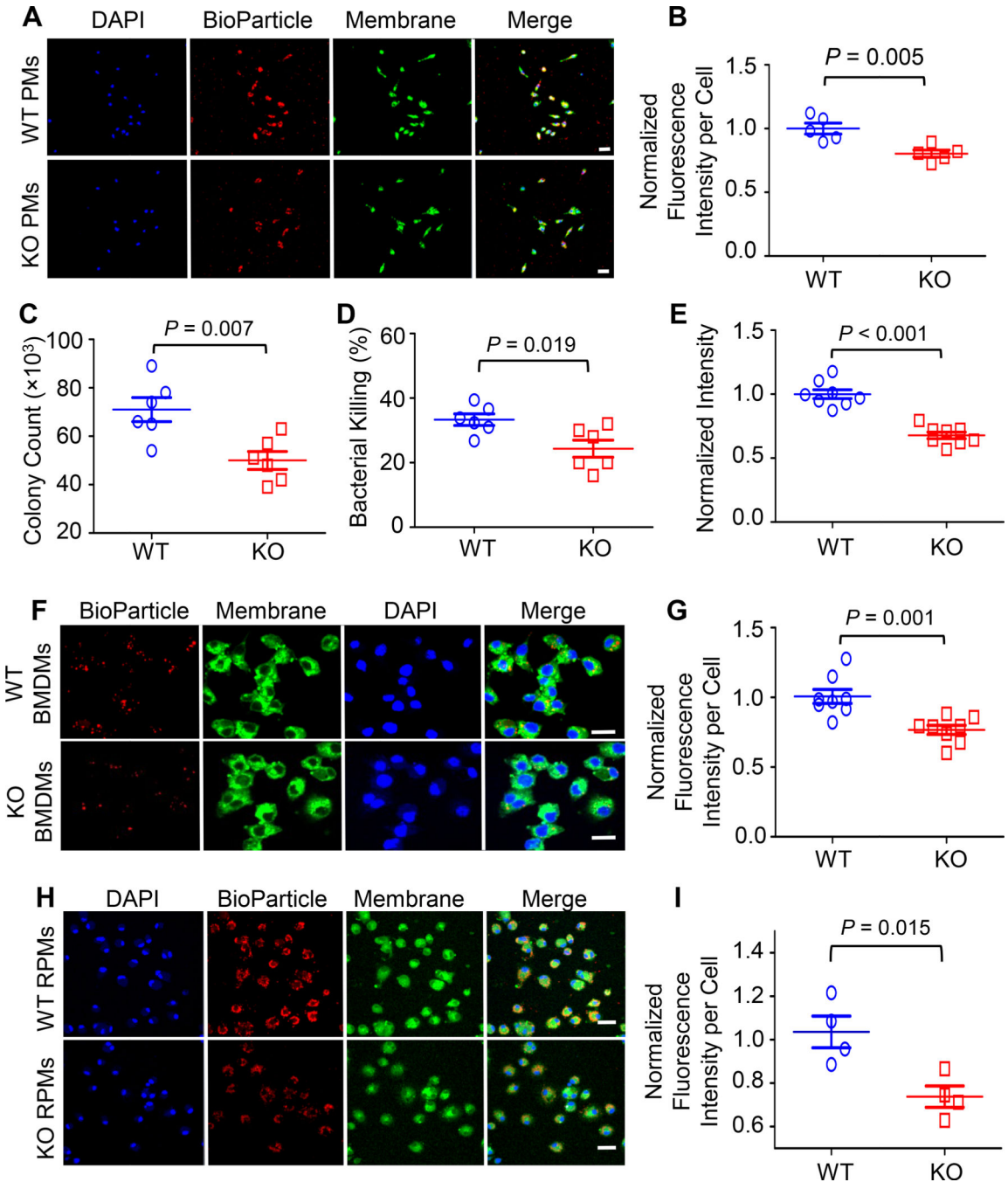

Figure 3. Sectm1a depletion suppresses phagocytic and bactericidal activities of macrophages.

(A-B) Phagocytosis assays of peritoneal macrophages isolated from WT and Sectm1a-KO mice were performed by incubating with red fluorescence-conjugated pHrodo™ *E. coli* bioparticles. (A) After 1h incubation, images from different fields were captured on a confocal microscope. Scale bar, 20 μm. (B) The mean of red fluorescence intensity in each cell was quantified with Image J and normalized to control. Results are shown as means ± SED of 250 cells per sample. n = 5. (C-D) The phagocytic activity and intracellular killing of BMDMs were compared between WT and Sectm1a-KO mice by challenging with mouse

serum-opsonized *E. coli*. (C) After 1-h infection, the number of bacteria phagocytized by macrophages (CFU) was determined by serial dilution of cell lysate and plating on LB agar plates. (D) After another 4-h incubation, the number of bacteria remained in cells was quantified with the same way and the killing percentages were calculated as described in material and methods. n = 6. (E-G) The phagocytic efficiency of BMDMs isolated from WT or Sectm1a-KO mice was compared by incubating with red fluorescence-conjugated pHrodo™ *E. coli* bioparticles. (E) The intensity of red fluorescence in each well was determined with microplate reader after 1-h incubation and normalized to control. n = 8. (F) Representative images were taken by confocal microscope. Scale bar, 20 μm. (G) The mean of red fluorescence intensity in each cell was quantified with Image J and normalized to control. Results are shown as means ± SEM of 250 cells per sample. n = 8. (H-I) The phagocytosis assays of RPMs isolated from WT and Sectm1a-KO mice were performed by incubating with red fluorescence-conjugated pHrodo™ *E. coli* bioparticles. (H) Images were captured using settings mentioned in above. Scale bar, 20 μm. (I) The mean of red fluorescence intensity in each cell was quantified with Image J and normalized to control. Results are shown as means ± SEM of 250 cells per sample. n = 4. Data are representative of two (A-D, H-I) or three (E-G) independent experiments. All results are presented as mean ± SEM and analyzed by student's t test.

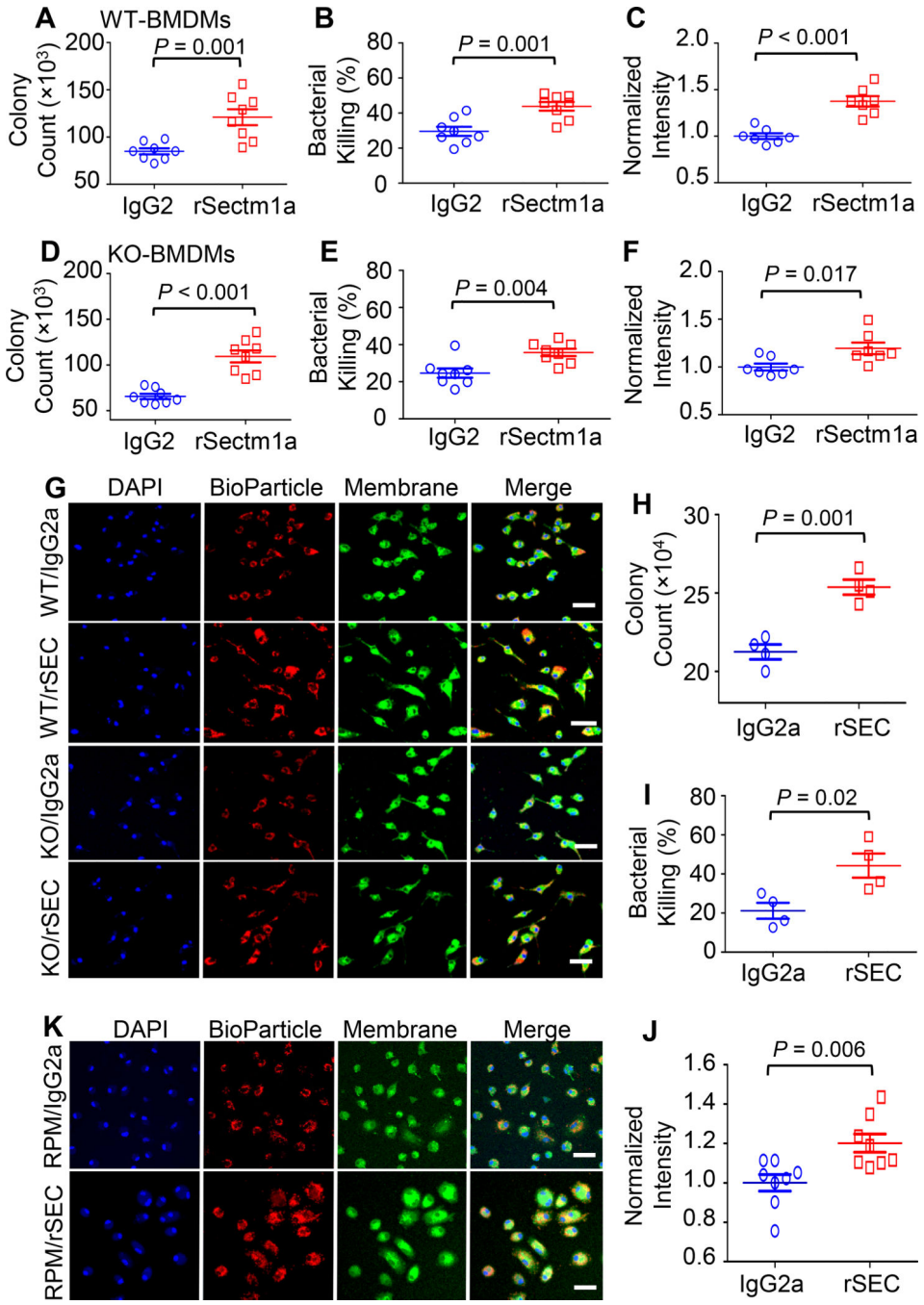

Figure 4. rSectm1a enhances phagocytosis and bactericidal capacity of macrophages.

Effects of rSectm1a (rSEC) on the phagocytic activity and bacterial killing were determined in BMDMs isolated from WT/KO mice and RPMs obtained from WT mice. All macrophages were pre-treated with rSectm1a (rSEC, 800 ng/ml) or IgG2a (500 ng/ml, stoichiometrically matched amount) for 20 h before incubating with mouse serum-opsonized *E. coli* or red fluorescence-conjugated pHrodo™ *E. coli* bioparticles. (A-C) rSectm1a treatment significantly increased the capacity of WT-BMDMs to phagocytize (A) and kill live *E. coli* (B). (C) Red fluorescence-conjugated pHrodo™ *E. coli* bioparticles were used to

confirm phagocytosis assay results. n =7–8. (D-F) The same design strategy was applied to BMDMs isolated from Sectm1a-KO mice. Pre-treatment with rSectm1a restored phagocytic (D) and killing (E) capacity of KO-BMDMs in response to live *E. coli* challenge. (F) The rSectm1a-induced increase in phagocytic capacity was confirmed using red fluorescence-conjugated pHrodo™ *E. coli* bioparticles. n =7–8. (G) Representative confocal images of phagocytosis assay in WT-BMDMs and KO-BMDMs with red fluorescence-conjugated pHrodo™ *E. coli* bioparticles. Scale bar, 20 μm. (H-J) rSectm1a significantly up-regulated the capacity of WT-RPMs to phagocytize (H) and kill live *E. coli* (I) (n = 4). (J) Red fluorescence-conjugated pHrodo™ *E. coli* bioparticles were used to confirm phagocytosis assay result with live bacterial (n = 8). (K) Representative confocal images of phagocytosis assay in WT-RPM with red fluorescence-conjugated pHrodo™ *E. coli* bioparticles. Scale bar, 20 μm. Data are representative of two (H-I) or three (A-F, J) independent experiments. All results are presented as mean ± SEM and analyzed by student's t test.

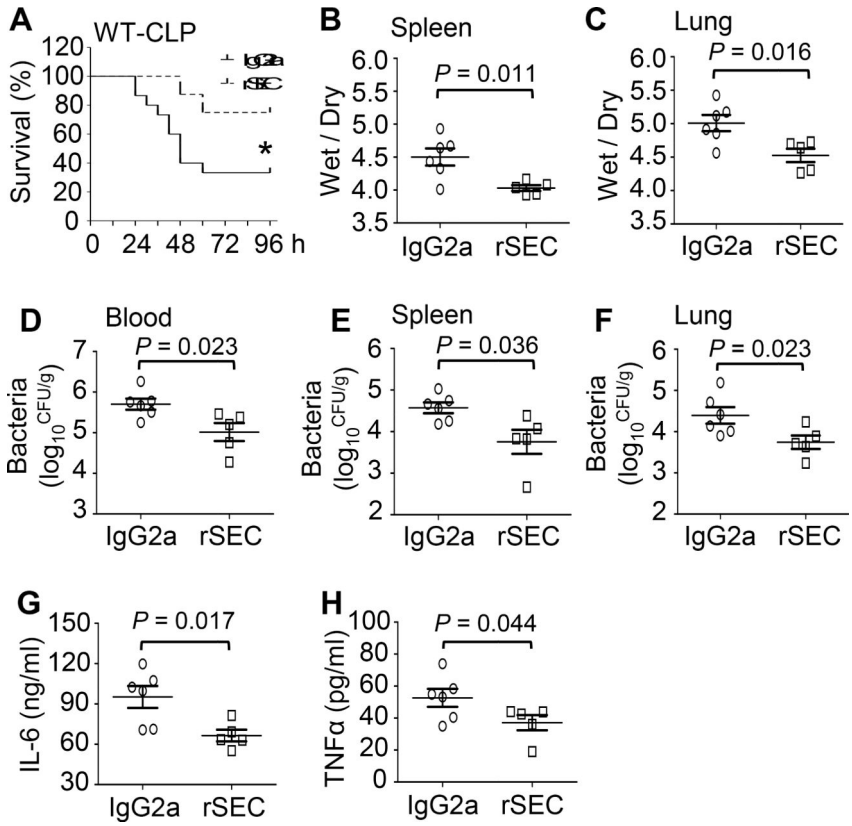

Figure 5. Administration of rSectm1a in CLP-mice decreases mortality, bacterial load, organ damage and systemic inflammation.

WT mice were subjected to a single *i.v.* dose of rSectm1a (rSEC: 300 μg/kg) or IgG2a (190 μg/kg, stoichiometrically matched amount) at 0.5 h post-CLP surgery. (A) Survival was monitored for 4 days (*, $P < 0.05$; n = 8 for rSectm1a-treated group, n=15 for IgG2a-treated group). (B and C) The spleen and lung tissues were collected from both IgG2a-treated and rSectm1a-treated mice at 24 h post-CLP, and wet weight to dry weight ratios of spleen (B) and lung (C) were quantified (n = 5–6). (D-F) Bacterial burdens in blood (D), spleen (E) and lung (F) were compared between two treatment groups at 24 h post-CLP (n = 5–6). (G-H) Serum levels of cytokines (G: IL-6 and H: TNFα) of two mouse groups were measured at 24 h after CLP surgery (n = 5–6). Data are representative of two independent experiments. The survival results were analyzed by Log-rank (Mantel-Cox) test. All other results are presented as mean ± SEM and analyzed by student's t test.

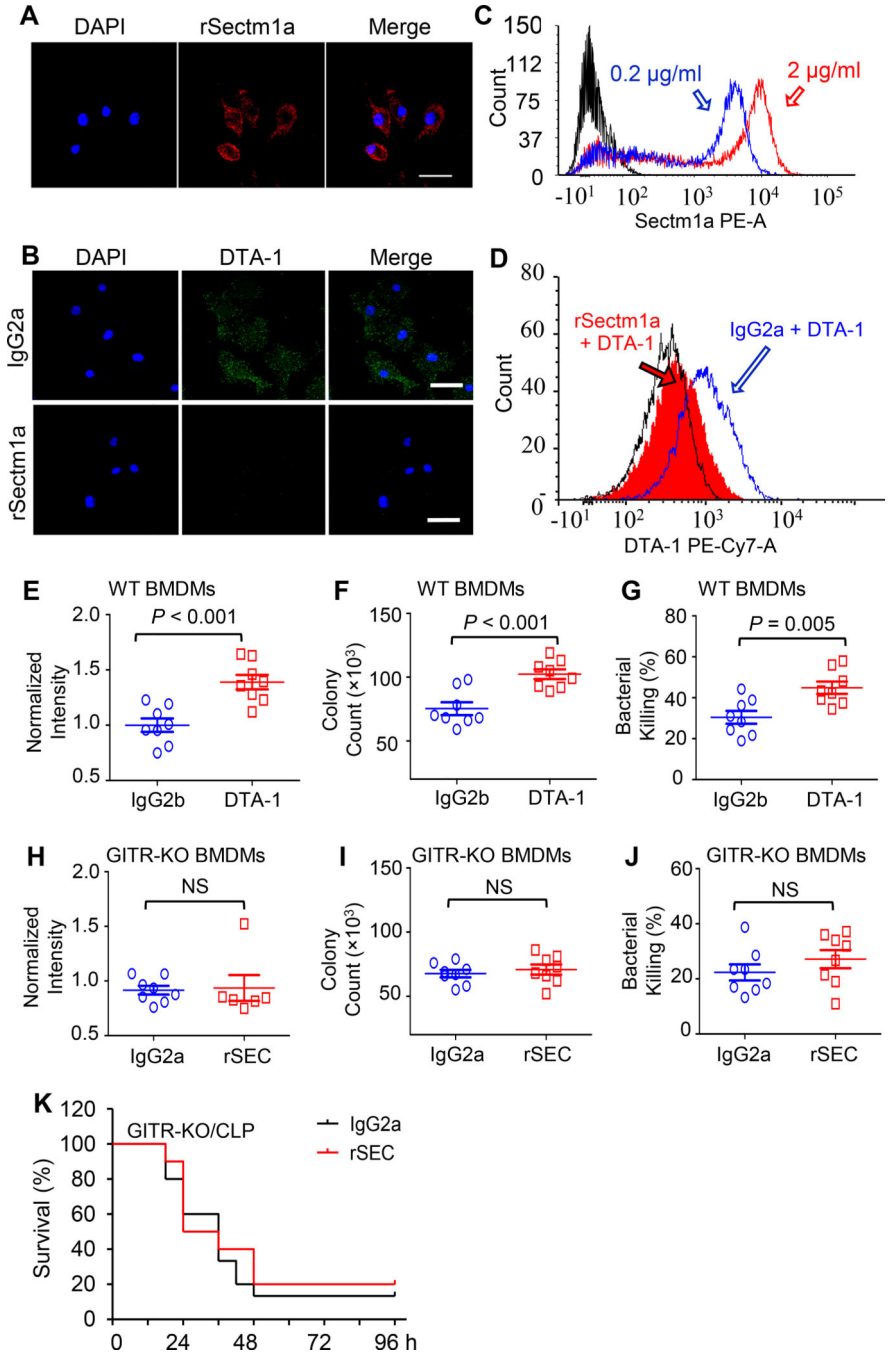

Figure 6. rSectm1a promotes bacterial uptake and clearance in macrophages through the activation of GITR.

(A) Immunofluorescence staining was used to determine whether rSectm1a cloud bind to the membrane of BMDMs. After blocking with 1% BSA, macrophages were incubated with rSectm1a which contains an immunoglobulin FC domain (IgG2a). After washing, the secondary antibody (anti-mouse IgG2a) conjugated with red fluorescence was applied to detect rSectm1a binding on the cell surface. (B) BMDMs were incubated with IgG2a (upper image) or rSECTM1A (lower image) before staining GITR with its antibody/ligand DTA-1 (Green). (C) The binding capability of rSectm1a to cell surface was further analyzed by

incubating with different concentrations of rSectm1a (0.2 μg/ml and 2 μg/ml), and flow cytometry analysis was used to determine the binding of rSectm1a to the cell membrane of BMDMs. (D) After blocking, BMDMs were incubated with IgG2a (1.5 μg/ml) or rSectm1a (2 μg/ml) before staining GITR with its antibody/ligand DTA-1 (2 μg/ml). The rSectm1a pre-incubation shifted back DTA-1 signal curve. (E-G) The effect of GITR activation on macrophage phagocytosis was determined after pre-treatment with DTA-1 (6 μg/ml) or IgG2b (4.5 μg/ml, stoichiometrically matched amount) for 20 h. After this, BMDMs were subjected to phagocytosis assay with *E. coli* BioParticle (E), live *E. coli* (F) and intracellular killing analysis (G), n = 8. (H-J) BMDMs were isolated from GITR-KO mice and incubated with IgG2a (500 ng/ml) or rSectm1a (800 ng/ml) for 20 h. Then, GITR-KO BMDMs were subjected to phagocytosis assay with *E. coli* BioParticle (H), live *E. coli* (I) and intracellular killing analysis (J), n = 6–8. (K) GITR-KO mice were subjected to a single *i.v.* dose of rSectm1a (300 μg/kg, n=10) or IgG2a (190 μg/kg, n=15) at 0.5 h post-CLP surgery, and survival was monitored for 4 days. Data are representative of two (A-D) or three (E-J) independent experiments. The survival results were analyzed by Log-rank (Mantel-Cox) test. All other results are presented as mean ± SEM and analyzed by student's t test or Mann-Whitney test.

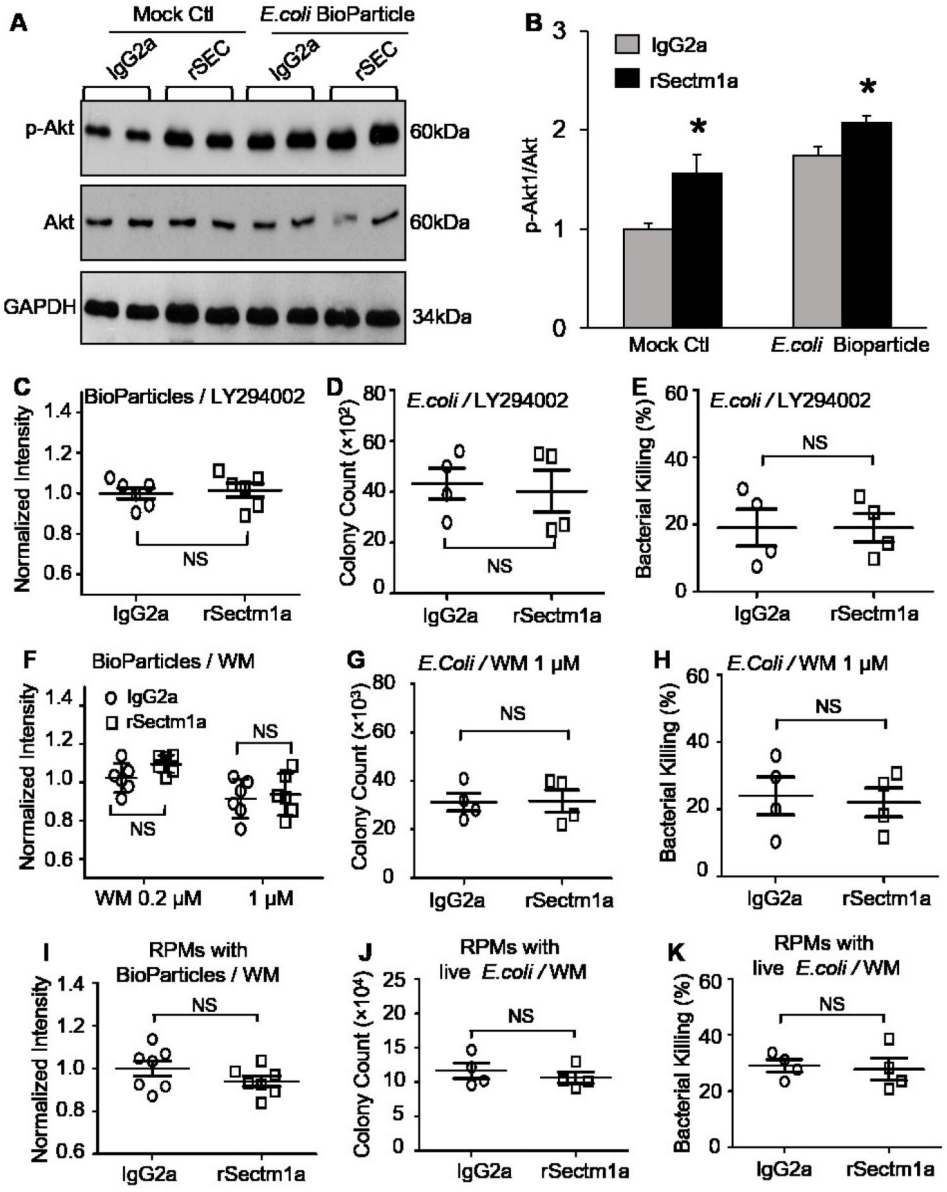

Figure 7. Pharmacologic inhibition of PI3K-Akt pathway abolishes the effects of rSectm1a on macrophage function.

(A-B) WT-BMDMs were pretreated with IgG2a (500 ng/ml) or rSectm1a (800 ng/ml) for 20 h, followed by treatment with or without *E. coli* BioParticle for 1 h. Then, cells were collected for Western-blotting analysis of total and phosphorylated Akt. Representative immuno-blots (A) and their quantification analysis results (B). GAPDH was used as a loading control. (*, $P < 0.05$; n=4). (C-E) The PI3K inhibitor, LY294002 (50 μM), was used to treat BMDMs for 0.5 h before stimulating with rSectm1a. After incubating with IgG2a (500 ng/ml) or rSectm1a (800 ng/ml), BMDMs were subjected to phagocytosis assay with *E. coli* BioParticle (C), live *E. coli* (D) and intracellular killing analysis (E), n = 4–6. (F-H) Another PI3K inhibitor, wortmannin (WM) (0.2 μM or 1 μM), was used to treat BMDMs for 0.5 h before stimulating with rSectm1a. After incubating with IgG2a (500 ng/ml) or rSectm1a (800 ng/ml), BMDMs were subjected to phagocytosis assay with *E. coli*

BioParticle (F). The phagocytosis (G) and intracellular killing assay (H) of live *E. coli* were conducted in BMDMs pretreated with WM (1 μM), n = 4–6. (I-K) The PI3K inhibitor, WM (1 μM), was used to treat RPMs for 0.5 h before stimulating with rSectm1a. After incubating with IgG2a (500 ng/ml) or rSectm1a (800 ng/ml), RPMs were subjected to phagocytosis assay with *E. coli* BioParticle (I), live *E. coli* (J) and intracellular killing analysis (K), n = 4–8. Data are representative of two independent experiments. All results are presented as mean ± SEM and analyzed by student's t test or two-way ANOVA.